David Sellmyer Publications   Research Papers in Physics and Astronomy

5-15-2005

Cluster-assembled exchange-spring nanocomposite permanent magnets

X. Rui
University of Nebraska - Lincoln

Zhiguang Sun
University of Nebraska - Lincoln, zsun3@unl.edu

Yinfan Xu
University of Nebraska - Lincoln, yxu2@unl.edu

David J. Sellmyer
University of Nebraska-Lincoln, dsellmyer@unl.edu

Jeffrey E. Shield
University of Nebraska - Lincoln, jshield@unl.edu

Follow this and additional works at: http://digitalcommons.unl.edu/physicssellmyer

Part of the Physics Commons

Cluster-assembled exchange-spring nanocomposite permanent magnets

X. Rui
Department of Mechanical Engineering, University of Nebraska, Lincoln, Nebraska 68588

Z. G. Sun and Y. Xu
Center for Materials Research and Analysis, University of Nebraska, Lincoln, Nebraska 68588

D. J. Sellmyer
Department of Physics and Astronomy, and Center for Materials Research and Analysis,
University of Nebraska, Lincoln, Nebraska 68588

J. E. Shield[a)]
Department of Mechanical Engineering, and Center for Materials Research and Analysis,
University of Nebraska, Lincoln, Nebraska 68588

(Presented on 11 November 2004; published online 13 May 2005)

Isotropic nanocomposite magnetic structures were produced via cluster assembly routes with energy products reaching 18 MG Oe. Gas aggregation produces Fe clusters with an average size less than 10 nm with a very narrow size distribution, and these were embedded in a hard magnetic matrix by cosputtering of FePt. Structures produced were crystallographically isotropic with Fe cluster phase content ranging from 0 to 30 vol %. The coercivity decreased from 13 kOe as Fe cluster content increased. Single-phase-type hysteresis loops indicating excellent exchange coupling at low Fe cluster content give way to a stepped demagnetization loop at an Fe cluster content greater than 20%. The energy product initially increased with Fe cluster content, then decreased. © *2005 American Institute of Physics*. [DOI: 10.1063/1.1853271]

INTRODUCTION

Nanocomposite exchange-spring permanent magnets have generated a significant amount of attention in the last dozen years. The combination of soft and hard magnetic phases, assembled at the nanoscale, results in high remanence and concomitant high energy products when compared to conventional, nonexchange-coupled permanent magnet materials.[1–3] For example, isotropic, noninteracting Nd–Fe–B-based magnets have energy products of 12–14 MG Oe and a theoretical maximum of 16 MG Oe.[4] Nanocomposite permanent magnets based in the same system have achieved energy products greater than 20 MG Oe,[5] and predictions based on modeling studies are more than twice that.[6] The magnetic performance is strongly tied to features of the nanostructure, primarily scale of the hard and soft magnetic phases and the phase morphology. Specifically, ideally the soft magnetic phase dimension is on the order of twice the domain wall width of the hard magnetic phase, or 5–10 nm.[1] Larger scale structures result in some of the soft magnetic phase remaining uncoupled. Magnetic reversal initiates in these uncoupled regions.[7] As a result, nonideal nanostructures lead to early reversal and lower-than-expected energy products. Consequently, there is a great deal of effort to control the nanostructural development. In melt-processed or devitrified materials, it has proven to be very difficult to generate appropriately fine and uniform nanostructures. In this article, we report cluster-assembled nanocomposite exchange-spring permanent magnets with extremely fine and uniform structures with excellent magnetic properties.

EXPERIMENTAL PROCEDURES

Clusters were fabricated by the gas-aggregation technique[8] in which Fe clusters are formed through collisions with the Ar ions. The atomic gas was produced by dc magnetron sputtering from a 99.9% pure Fe target. The base pressure of the system was below 10^{-7} Torr, and an Ar/He gas mixture was introduced into the nucleation chamber. He gas was used to ensure uniform temperature in the nucleation chamber. The He gas flow rate was varied from 250 to 300 sccm while the Ar gas flow rate was varied between 250 and 350 sccm. The sputtering power also influences cluster size and size distribution. In this study, it was varied between 60 and 160 W, although most depositions were done at a power level of 160 W.

The gas aggregation system is also equipped with a second dc magnetron sputtering source, and an ac magnetron sputtering source, both currently situated perpendicular to the cluster source. The ac source was used to deposit a C overlay to protect the deposited material from oxidation. The dc source was used to deposit hard magnetic FePt thin films, and alternating deposition between the cluster gun and the second dc magnetron gun allowed the development of nanocomposite structures, with the clusters imbedded in the hard magnetic phase. The nanocomposite structures were fabricated by alternating deposition of FePt and Fe clusters by physically rotating the substrate for deposition from the cluster or thin film source. The relative fraction of Fe clusters and FePt film was controlled by varying deposition times from each source. The relative volume fraction of each phase was determined from the respective sputtering rates and the deposition times, and the accuracies were on the order of 10%. The material was deposited directly on a carbon sup-

[a)]Electronic mail: jshield2@unl.edu
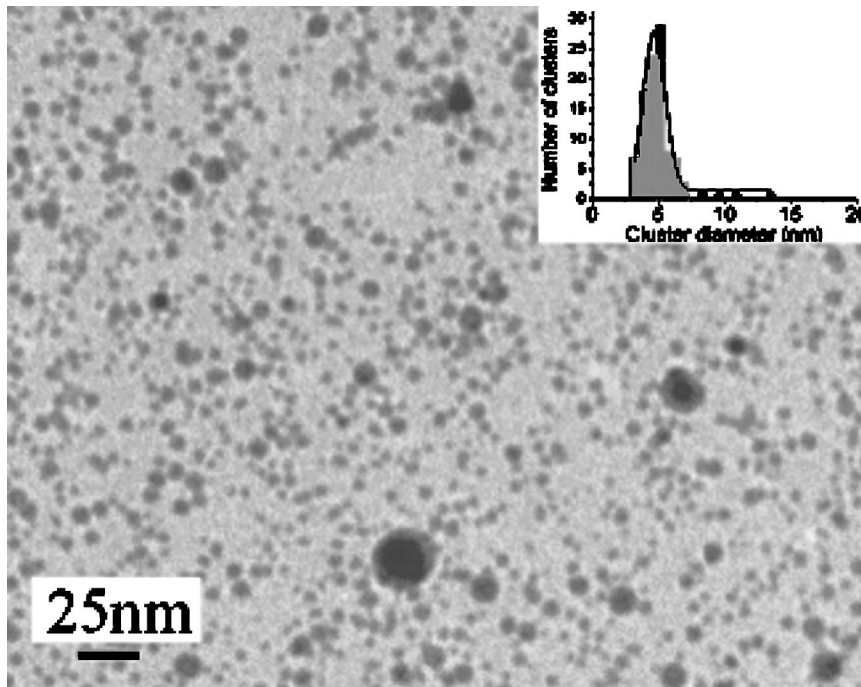
97, 10K310-1

FIG. 1. Fe clusters formed by gas aggregation deposited directly on a graphite support film. The inset shows the cluster size distribution.

port grid for transmission electron microscopy and, simultaneously, a Si substrate for characterization by x-ray diffraction and magnetometry.

The clusters and nanocomposite structures were characterized by transmission electron microscopy using a JEOL2010 transmission electron microscope operating at 200 kV, x-ray diffraction using a Rigaku diffractometer, and magnetometry using a Quantum Design MPMS superconducting quantum interference device and alternating gradient field magnetometers. The magnetic signal from the substrate was subtracted from the nanocomposite magnetic signal by fitting a straight line to the high-field region and subtracting the linear portion from the measured signal. In this article, we present results for in-plane measurements only. As such, the demagnetization factor was assumed to be zero.

RESULTS AND DISCUSSION

The cluster size and size distribution were critically dependent on the processing parameters, primarily the gas flow rates, which controlled the frequency of collisions during the cluster formation process. Fe clusters with an average size from 5 to 20 nm were produced with extremely narrow size distributions. For example, clusters with an average size of 4.7 nm and a σ/d of approximately 0.1, where σ is the standard deviation and d is the average cluster size, are shown in Fig. 1. The narrow size distribution essentially creates a monosized nanostructure with respect to the α-Fe phase. This is in direct comparison to σ/d values of 0.2–0.3 in nanostructures produced by rapid solidification.[9] Electron diffraction patterns revealed that the clusters formed in the bcc structure.

The as-deposited FePt film was in the disordered $A1$ fcc structure. Therefore, heat treatments were necessary to form the hard magnetic $L1_0$ structure. Rapid thermal annealing was utilized for the heat treatment. This processing limits the exposure of the film to high temperatures, reducing interdif-

fusion between the FePt matrix and Fe clusters, as well as coarsening of the FePt structure that can deleteriously affect the magnetic properties. The magnetic properties, and thus the formation of the $L1_0$ structure, were sensitive to the exact heat treatment. The optimum heat treatment was found to be 600 °C for 10 min, which resulted in a coercivity of greater than 10 kOe for FePt thin film structures with no Fe clusters. The films showed predominantly isotropic grain orientations, as deduced from x-ray diffraction analysis and comparison of in- and out-of-plane magnetic measurements.

Different phase contents in the nanocomposite structures were achieved by varying the deposition times for the Fe clusters and FePt thin films. Nanocomposite structures containing between 0 and 30 vol % Fe clusters were fabricated. Figure 2 shows a typical nanocomposite structure before heat treatment to form the $L1_0$ structure. This image shows Fe clusters and a background of fine FePt grains prior to heat treatment. This image is of a single layer of Fe clusters and FePt; multiple layers were used to form the nanocomposite structures. The heat treatment results in a coarsening of the very fine FePt structure.
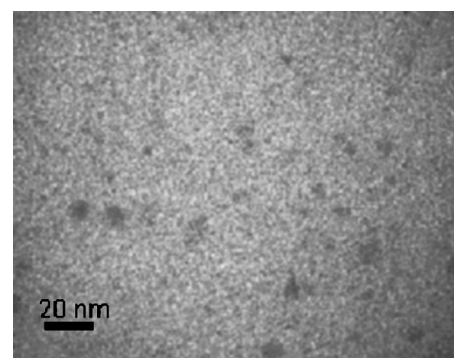

FIG. 2. Transmission electron microscopy micrograph showing the nanocomposite FePt/Fe cluster system prior to heat treatment. The Fe cluster size was on the order of 6 nm.
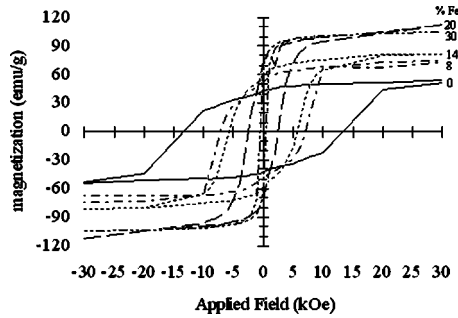
FIG. 3. Hysteresis curves at 300 K for the nanocomposite films with different Fe cluster content. All samples were annealed at 600 °C/10 min prior to measurement.

The magnetic behavior of the FePt and FePt/Fe cluster nanocomposites was also evaluated. Figure 3 shows hysteresis curves for the various samples. A smooth demagnetization curve was observed for the films containing 8 and 14 vol % Fe clusters, indicating excellent exchange coupling between the FePt matrix and Fe clusters. In the film with 20 % Fe clusters, a step in the demagnetization loop, indicating two-phase behavior, was observed. The problem may be that the Fe clusters are "clustering" during deposition, leading to regions with effectively larger Fe regions and thus decoupled from the hard magnetic matrix. This two-phase behavior may also develop due to compositional changes in the FePt phase that arise due to different Fe and Pt sputtering rates. A FePt film with no Fe clusters deposited after the 20 vol % Fe cluster nanocomposite displayed a large step in the demagnetization loop. Further work to better maintain compositional control over the FePt phase is underway.

The overall magnetic properties of the FePt and FePt/Fe cluster nanocomposite structures are summarized in Fig. 4.
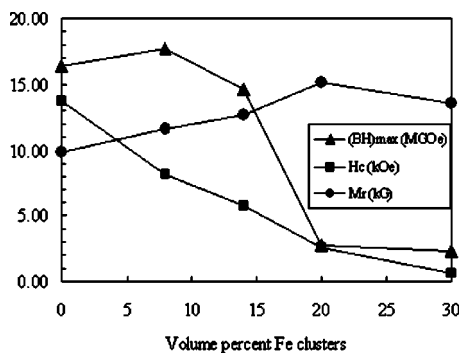

FIG. 4. Summary of magnetic properties of nanocomposite films.

The FePt $L1_0$ film, with no Fe clusters, exhibited a coercivity of greater than 10 kOe, and the coercivity decreased systematically with increasing Fe cluster content, as might be expected. The remanence increased systematically with Fe cluster content, while the energy product went through a maximum of 17.7 MG Oe. The energy products were well above those expected for randomly oriented, noninteracting magnetic systems. For example, isotropic, single-phase, non-interacting FePt has a theoretical maximum of 12.8 MG Oe. The enhanced energy products are attributed to exchange-spring interactions between the hard magnetic FePt $L1_0$ phase and the soft magnetic Fe clusters.

CONCLUSIONS

This work shows that nanocomposite structures can be achieved with excellent control of scale and phase fraction through cluster assembly processes utilizing codeposition processing. Soft magnetic Fe cluster formation by gas aggregation techniques produces cluster sizes below 10 nm. Nanocomposite α-Fe/FePt structures can be achieved through codeposition of Fe clusters and FePt thin films, resulting in outstanding energy products for isotropic structures. The magnetic properties strongly depend on the phase content of the FePt/Fe clusters nanocomposites. Energy products on the order of 18 MG Oe were realized in the two-phase system, and were increased over single-phase materials. The coercive force decreased with increasing Fe cluster content, but were reasonably high (5.7 kOe) at 14 vol % Fe clusters.

ACKNOWLEDGMENT

[1]E. F. Kneller and R. Hawig, IEEE Trans. Magn. **27**, 3588 (1991)

[2]R. Skomski and J. M. D. Coey, Phys. Rev. B **48**, 15812 (1993).

[3]R. Fischer, T. Schrefl, H. Kronmuller, and J. Fidler, J. Magn. Magn. Mater. **150**, 329 (1995).

[4]B. M. Ma, J. W. Herchenroeder, B. Smith, M. Suda, D. N. Brown, and Z. Chen, J. Magn. Magn. Mater. **219**, 418 (2002).

[5]J. Bernardi, *et al.*, J. Magn. Magn. Mater. **219**, 186 (2000).

[6]R. Fischer, T. Schrefl, H. Kronmuller, and J. Fidler, J. Magn. Magn. Mater. **150**, 329 (1995).

[7]Y. Gao, D. Shindo, and A. K. Petford-Long, J. Appl. Phys. **93**, 8119 (2003).

[8]D. J. Sellmyer, C. P. Luo, Y. Qiang, and J. P. Liu, in *Handbook of Thin Films*, *Nanomaterials and Magnetic Thin Films* Vol. 5, edited by H. S. Nalwa (Academic, New York, 2002), p. 337.

[9]J. E. Shield, Y. Liu, R. Marr, Z. Chen, and B. M. Ma, IEEE Trans. Magn. **40**, 2901 (2004).